CELL CYCLE
2017, VOL. 16, NO. 16, 1502–1508
https://doi.org/10.1080/15384101.2016.1249548

Taylor & Francis
Taylor & Francis Group

REPORT

Eradication of melanoma *in vitro* and *in vivo* via targeting with a Killer-Red-containing telomerase-dependent adenovirus

Kiyoto Takehara[a,b,c], Shuya Yano[a,b,c], Hiroshi Tazawa[d], Hiroyuki Kishimoto[c], Nobuhiro Narii[e], Hiroyuki Mizuguchi[e], Yasuo Urata[f], Shunsuke Kagawa[c], Toshiyoshi Fujiwara[c], and Robert M. Hoffman[a,b]

[a]AntiCancer, Inc., San Diego, CA, USA; [b]Department of Surgery, University of California San Diego, San Diego, CA, USA; [c]Department of Gastroenterological Surgery, Okayama University Graduate School of Medicine, Dentistry and Pharmaceutical Sciences, Okayama, Japan; [d]Center for Innovative Clinical Medicine, Okayama University Hospital, Okayama, Japan; [e]Laboratory of Biochemistry and Molecular Biology, Graduate School of Pharmaceutical Sciences, Osaka University, Osaka, Japan; [f]Oncolys BioPharma, Inc., Tokyo, Japan

ABSTRACT

Melanoma is a highly recalcitrant cancer and transformative therapy is necessary for the cure of this disease. We recently developed a telomerase-dependent adenovirus containing the fluorescent protein Killer-Red. In the present report, we first determined the efficacy of Killer-Red adenovirus combined with laser irradiation on human melanoma cell lines *in vitro*. Cell viability of human melanoma cells was reduced in a dose-dependent and irradiation-time-dependent manner. We used an intradermal xenografted melanoma model in nude mice to determine efficacy of the Killer-Red adenovirus. Intratumoral injection of Killer-Red adenovirus, combined with laser irradiation, eradicated the melanoma indicating the potential of a new paradigm of cancer therapy.

ARTICLE HISTORY
Received 23 September 2016
Revised 11 October 2016
Accepted 12 October 2016

KEYWORDS
adenovirus; killer-red; melanoma; nude mouse; photodynamic therapy; telomerase

Introduction

Melanoma is a recalcitrant cancer. Melanoma accounts for only 1% of all skin cancer cases but most of skin cancer deaths. The rates of melanoma deaths have been rising for the last 30 y.[1]

Melanoma is resistant to conventional chemotherapy or radiotherapy. Metastatic melanoma represents a significant clinical problem because of inherent properties of the tumor and its interaction with the host.[2]

Novel strategy for therapy of melanoma such as immunotherapy, gene therapy, and molecularly-targeted therapy, which include BRAF inhibitors and anti-PD-1/PD-L1 antibodies has been developed.[3-5] We have recently demonstrated the efficacy of Trametinib (TRA) on a BRAF-V600E mutant patient-derived orthotopic xenograft (PDOX) nude mouse model.[6]

Photodynamic therapy (PDT) of cancer uses photosensitizers that can accumulate in tumors and subsequent light irradiation.[7,8] Specific-wavelength light irradiation induces photosensitizer-mediated generation of reactive oxygen species (ROS) and subsequent cytotoxicity. Although PDT has been applied in clinical settings for non-melanoma skin cancers, PDT has not been established as a standard therapy for cutaneous melanoma despite the promising results of past clinical trials.[3,5]

Our laboratory has developed PDT using expression of fluorescent proteins by cancer cells.[9-13]

Recently, we reported a novel PDT strategy with genetically encoded photosensitizer Killer-Red delivered with a telomerase-dependent adenovirus-mediated delivery system.[14] Killer-Red is an engineered dimeric red fluorescent protein obtained from a green fluorescent protein (GFP) homolog. Killer-Red generates reactive oxygen species (ROS) upon green light irradiation with a fluorescence excitation/emission maxima at 585/610 nm and effects phototoxicity on cancer cells.[15]

The present report evaluates the efficacy of Killer-Red adenovirus on human melanoma cells *in vitro* and in orthotopic nude-mouse models.

Results and discussion

In vitro *anti-tumor efficacy of killer-red with light irradiation*

Human malignant melanoma Mel526-GFP and FEMX1-GFP cells infected with Killer-Red adenovirus at a multiplicity of infection (MOI) of 10 expressed red fluorescence 48 h after infection. After laser irradiation for 30 min, Killer-Red-infected cells showed significant morphological changes, including cell-membrane destruction and photobleaching, whereas non-infected cells did not show any changes after irradiation (Fig. 1A). Killer-Red-adenovirus-infected cells showed a decrease in cell viability in a dose-dependent manner. There was a significant decrease in cell viability of irradiated cells compared with non-irradiated cells at all doses of virus tested (Fig. 1B) ($P < 0.05$). Mel526-GFP cells, infected with Killer-Red adenovirus at an MOI of 10, showed an irradiation time-dependent decrease of GFP fluorescence and cell viability (Fig. 2).

In vivo *efficacy of Killer-Red adenovirus PDT*

Killer-Red adenovirus was injected at a dose of 5.0×10^7 plaque-forming units (PFU)/50 μl into the Mel536-GFP melanoma

CONTACT Toshiyoshi Fujiwara toshi_f@md.okayama-u.ac.jp Department of Gastroenterological Surgery, Okayama University Graduate School of Medicine, Dentistry and Pharmaceutical Sciences,2-5-1 Shikata-cho, Kita-ku, Okayama 700-8558, Japan; Robert M. Hoffman, Ph.D. all@anticancer.com AntiCancer, Inc, 7917 Ostrow Street, San Diego, CA 92111, USA.

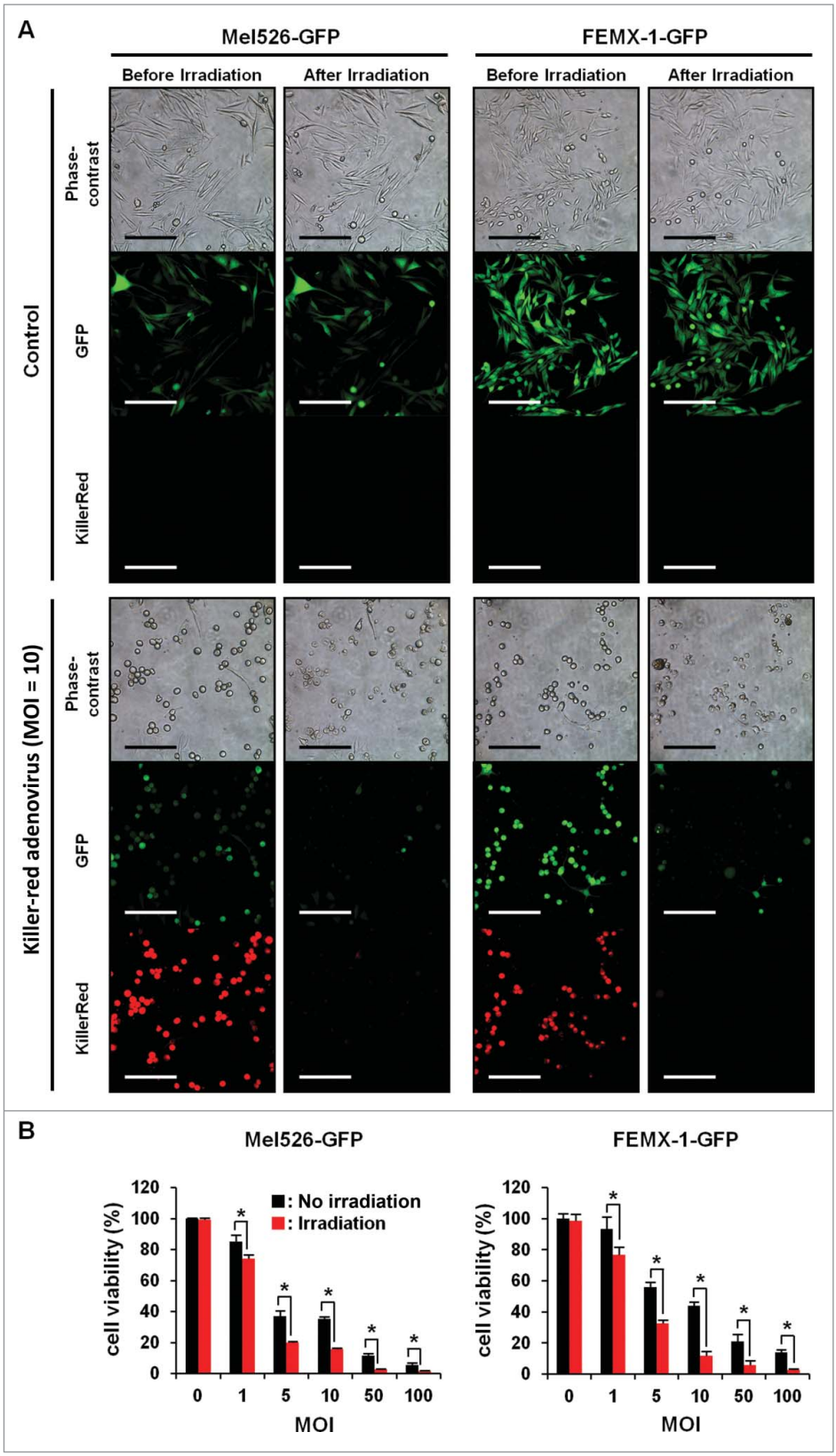

Figure 1. Light irradiation decreased cell viability of human melanoma cells infected with Killer-Red adenovirus. Mel526-GFP and FEMX-1-GFP cells were infected with Killer-Red adenovirus at an MOI of 10. 48 h after infection, the virus-infected cells were irradiated with a 589 nm laser for 30 min. Scale bar: 200 μm. B, Mel526-GFP and FEMX-1-GFP cells were infected with Killer-Red adenovirus at the indicated MOIs for 48 h. Cell viability was evaluated using a tetrazolium-based assay immediately after laser irradiation. Cell viability was calculated relative to that of the mock-infected group, which was set at 100%. Cell viability data are expressed as mean values $\pm$ SD (n = 3). Statistical significance was determined using the Student's *t*-test. *, $P < 0.05$.

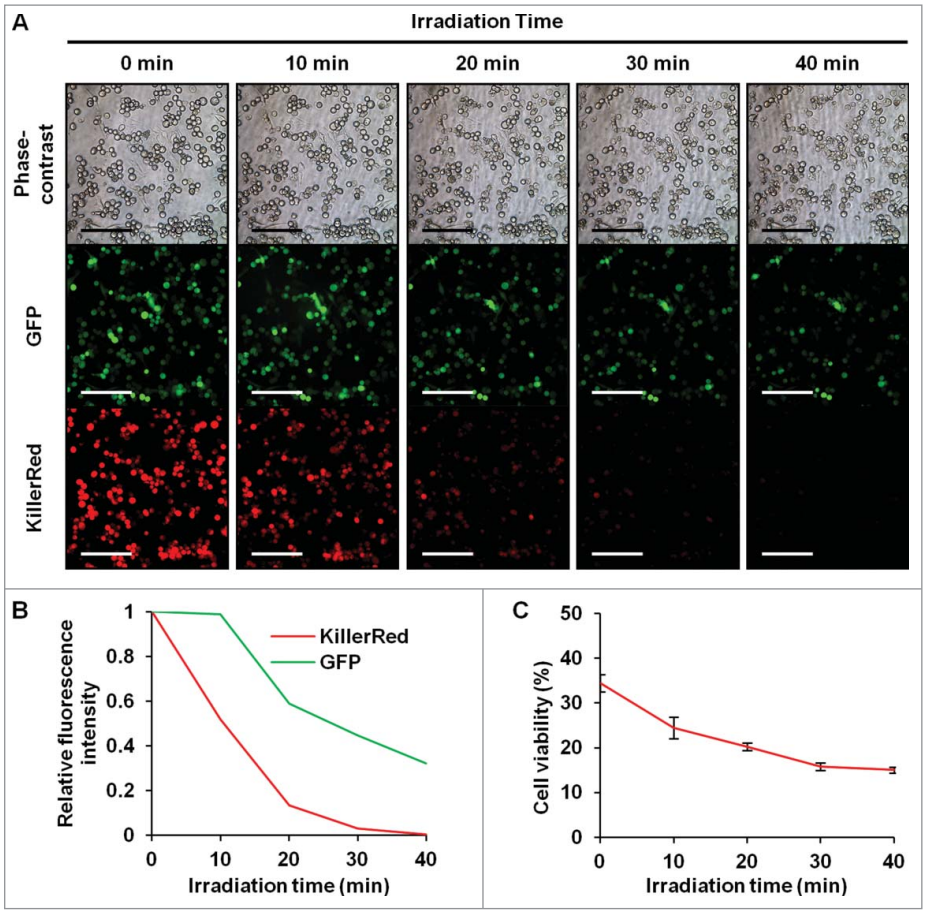

Figure 2. Time-course observation of laser-irradiated Mel526-GFP cells infected with Killer-Red adenovirus. (A) Irradiation-time-dependent decreased GFP fluorescence of Killer-Red adenovirus-infected Mel526-GFP cells. Scale bar: 200 μm. (B, C) Irradiation time-dependent decrease of GFP and Killer-Red fluorescence intensity (B) and cell viability (C) Mel526-GFP cells were infected with Killer-Red adenovirus at an MOI of 10 for 48 h, and cell viability was determined using the WST-8 assay immediately after laser irradiation for 10, 20, 30, or 40 min. Cell viability was calculated relative to that of the mock-infected group, which was set at 100%. Fluorescence intensity was measured using Image J software. Relative fluorescence intensity was calculated relative to that of non-irradiated cells, which was set at 1. Cell viability data are expressed as mean values ± SD (n = 3). Statistical significance was determined using the Student's *t*-test. *, $P < 0.05$.

growing subcutaneously. Three days after virus injection, Killer-Red-mediated red fluorescence was clearly observed in the infected tumor (Fig. 3). Photodynamic therapy (PDT) was performed using a 589 nm diode pumped solid state laser. Tumors were irradiated with the laser (300 mW/cm^2) for 45 min at each session. Virus was injected on days 0, 7 and 14 and laser irradiation was performed on days 3 and 4, 10 and 11, and 17 and 18.

Killer-Red adenovirus with laser irradiation regressed the tumor (Fig. 4). The combination therapy of Killer-Red adenovirus and laser irradiation apparently eradicated the tumors as determined both by tumor volume and fluorescence intensity ($P < 0.05$) (Fig. 5).

Pigmentation and other therapeutic-resistance mechanisms seem to limit the therapeutic effect of PDT for melanoma.[5] Our results clearly demonstrated the therapeutic efficacy of Killer-Red-adenovirus-based PDT for cutaneous melanoma. A telomerase-specific conditionally Killer-Red-expressing adenovirus has some advantages compared with conventional PDT: (a) the high tumor selectivity and prolonged accumulation of Killer-Red, which is achieved by using a telomerase-specific replicating adenovirus; (b) the dual effects mediated by Killer-Red-mediated cell death as well as virus-mediated cell death.[14] Since light in the yellow-green to orange wavelength range for excitation of Killer-Red has limited depth penetration,[8] cutaneous melanoma can be a good indication for Killer-Red-based PDT. We previously reported that intra-tumor injection of a telomerase-specific replication-competent adenovirus (OBP-301) eliminated lymph node metastasis of an orthotopic colorectal cancer model.[16,17] These findings suggest that Killer-Red adenovirus may also be effective for eradicating potential lymph node metastasis of melanoma.

Killer-Red adenovirus has potential for neo-adjuvant therapy followed by fluorescence-guided surgery of melanoma.[18-23] Future experiments will also utilize intravenous or i.p. administration of Killer-Red adenovirus for therapy of disseminated disease.

The presence or absence of melanin may affect the therapeutic outcome of melanoma.[24-26]

Previously-developed concepts and strategies of highly-selective tumor targeting can take advantage of molecular targeting of tumors, including tissue-selective therapy which focuses on unique differences between normal and tumor tissues.[27-32]

Materials and methods

Cell lines

Green fluorescent protein-expressing human malignant melanoma cell lines Mel526-GFP and FEMX1-GFP (AntiCancer, Inc., San Diego, CA) were maintained and cultured in

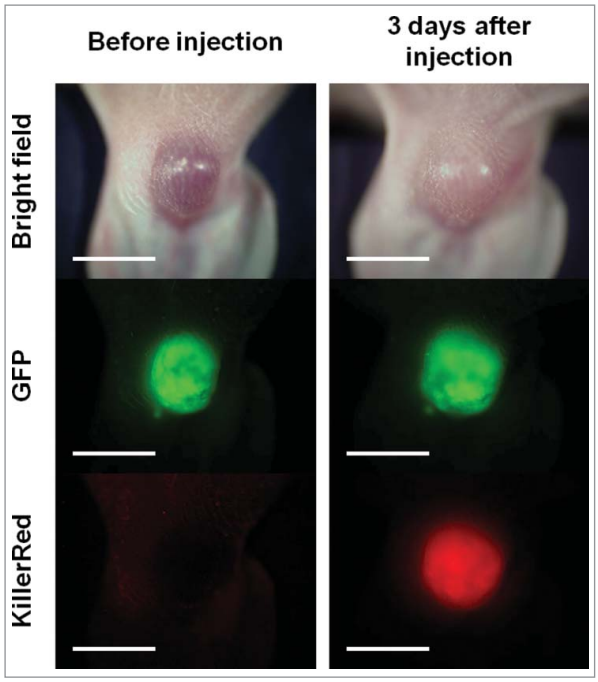

Figure 3. Expression of red fluorescence of Killer-Red in orthotopic Mel526-GFP melanoma 3 d after intratumor injection of Killer-Red adenovirus. Scale bar: 5 mm.

Dulbecco's modified Eagle's medium (DMEM) with 10% fetal bovine serum, 100 U/ml penicillin and 100 mg/ml streptomycin. The cells were routinely maintained at 37°C in a humidified atmosphere with 5% CO_2. These cells lines produce melanin.

Killer-Red-expressing telomerase-specific adenovirus

The Killer-Red gene[14] was incorporated in a conditionally-replicating adenovirus, in which the promoter element of the human telomerase reverse transcriptase (hTERT) gene drives the expression of *E1A* and *E1B* genes linked with an internal ribosome entry site (IRES). The Killer-Red gene was inserted under the CMV promotor into the E3 region.[14] The Killer-Red adenovirus was purified using cesium chloride step gradients with titers determined by a plaque-forming assay using 293 cells. The virus was stored at −80°C.

Cell viability assay

Cells were seeded on 96-well plates at a density of 3×10^3 cells/well 24 h before infection and were infected with Killer-Red adenovirus at MOIs of 0, 1, 5, 10, 50, or 100 plaque-forming units (PFU)/cell. Cells were irradiated with a 589 nm diode pumped solid state laser (Changchun New Industries Optoelectronics Technology Co., Ltd., Changchun, P.R. China) (300 mW/cm^2) for 30 min, 48 h after virus infection. Cell viability was determined immediately after irradiation using the Cell Counting Kit-8 (Dojindo, Kumamoto, Japan), which is based on a (2-(2-methoxy-4-nitrophenyl)-3-(4-nitrophenyl)-5-(2,4-disulfophenyl)-2H-tetrazolium) assay, according to the manufacturer's protocol.

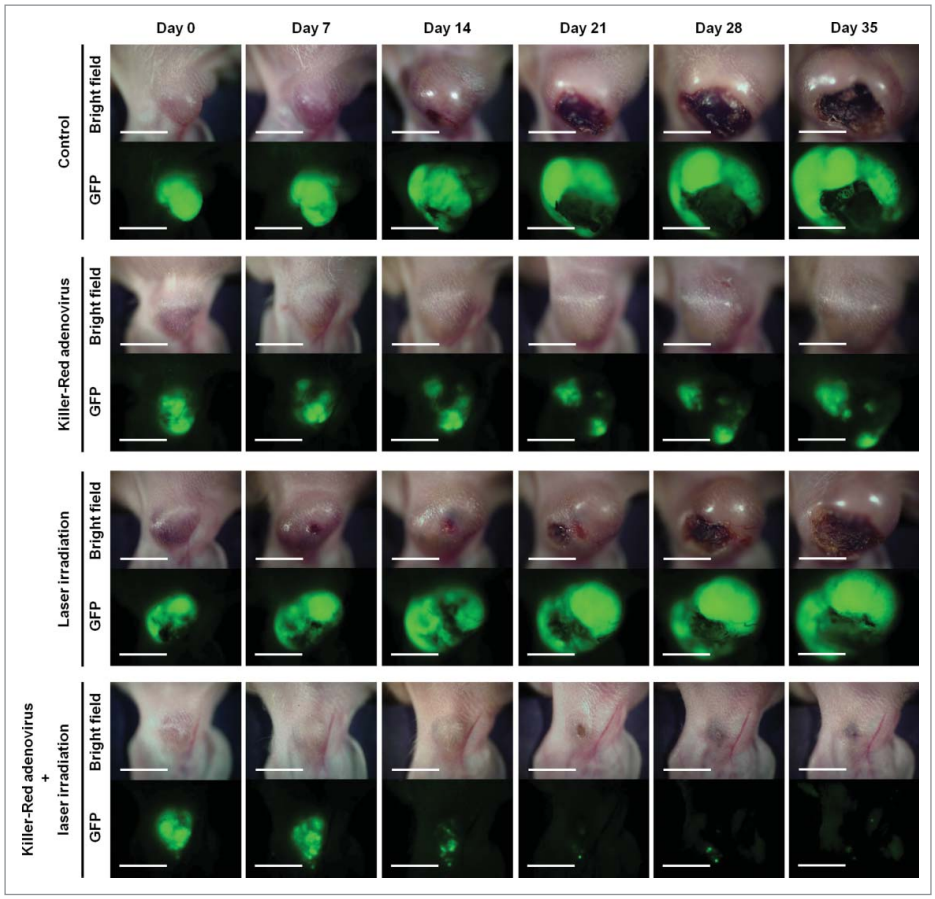

Figure 4. Time course macroscopic images of orthotopic Mel526-GFP melanoma, with no treatment, treated with Killer-Red only, laser irradiation only and Killer-Red followed by laser irradiation. Scale bar: 5 mm.

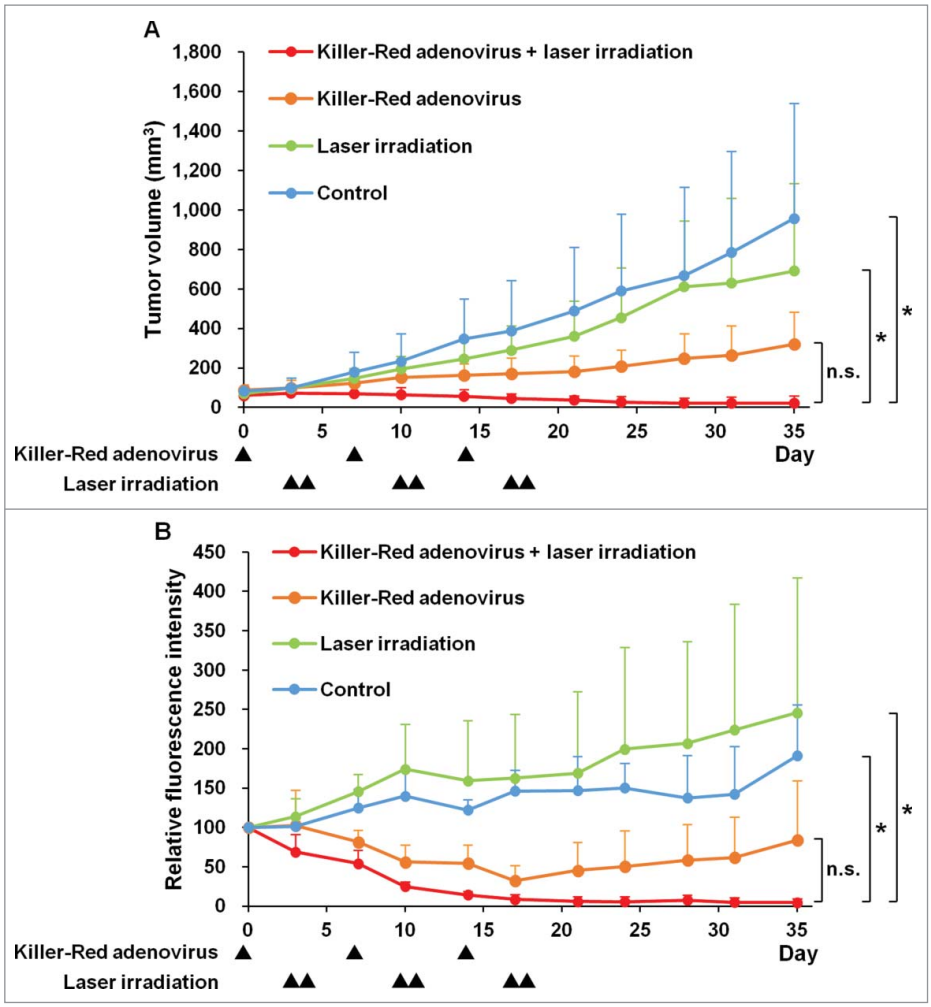

Figure 5. Efficacy of Killer-Red adenovirus combined with laser irradiation in the orthotopic Mel526-GFP melanoma model. (A) Tumor growth curves of orthotopic Mel526-GFP melanoma model. Tumor growth is expressed as the mean tumor volume ± SD. (B) Relative GFP fluorescence intensity of Mel526-GFP tumors. Relative fluorescence intensity of tumors at each day was calculated relative to that of day 0, which was set at 100. Relative fluorescence intensity is expressed as the mean relative fluorescence intensity ± SD. *$p < 0.05$.

Cell viability of Killer-Red adenovirus-infected cells was calculated as the percentage of viable infected cells divided by that of viable non-infected cells.

Animal experiments

Athymic (nu/nu) nude mice (AntiCancer, Inc., San Diego, CA) were maintained in a barrier facility under HEPA filtration and fed with autoclaved laboratory rodent diet (Tecklad LM-485; Harlan Labs., Hayward, CA). All animal studies were conducted in accordance with the principles and procedures outlined in the National Institute of Health Guide for the Care and Use of Laboratory Animal under Assurance Number A3873-01.

Orthotropic melanoma model

Mel526-GFP cells (5×10^5 cell) suspended in 20 μl Matrigel^{TM} basement membrane matrix (BD biosciences, Bedford, MA) were injected between the skin and cartilage on the dorsal side of the left ear of 6-week-old athymic nude mice.[33] All animal procedures were performed under anesthesia with subcutaneous injection of ketamine (31.25 mg/kg), xylazine (6.25 mg/kg) and acepromazine (1.25 mg/kg). When the tumors grew to a diameter of 5 to 6 mm, Killer-Red adenovirus was injected intra-tumorally at 5.0×10^7 PFU/50 μl.

Killer-Red photodynamic therapy

Photodynamic therapy (PDT) was performed using the 589 nm diode pumped solid state laser. Tumors were irradiated with the laser (300 mW/cm^2) for 45 min at each session. Virus was injected on days 0, 7 and 14 and laser irradiation was performed on days 3 and 4, 10 and 11, and 17 and 18. The perpendicular diameter of each tumor was measured every 3 or 4 d, and tumor volume was calculated using the following formula: tumor volume (mm^3) $= a \times b^2 \times 0.5$, where a is the longest diameter, b is the shortest diameter, and 0.5 is a constant for calculation of the volume of an ellipsoid.

In vivo *imaging*

The OV100 small animal imaging system (Olympus Corp., Tokyo, Japan), was used. The OV100 contains an MT-20 light

source (Olympus Biosystems, Planegg, Germany) and DP70 CCD camera (Olympus), for whole body, as well as sub-cellular imaging in live mice.[34-36] Optics of the OV100 have been specially developed for macro-imaging as well as micro-imaging with high light-gathering capacity. Four individually-optimized objective lenses, parcentered and parfocal, provide a 105-fold magnification range. High-resolution images were captured directly on a PC (Fujitsu Siemens, Munich, Germany). Images were processed for contrast and brightness and analyzed with the use of Paint Shop Pro 8 and CellR.[37]

Statistical analysis

Data are shown as means ± SD. For comparison between 2 groups, significant differences were determined using the Student's *t*-test. For comparison of more than 2 groups, significant differences were determined using one-way analysis of variance (ANOVA) followed by a Bonferroni multiple group comparison test. Statistical significance was defined when the *P* value was less than 0.05.

Disclosure of potential conflicts of interest

Y. Urata is President & CEO of Oncolys BioPharma, Inc., the manufacturer of the killer-red adenovirus. H. Tazawa and T. Fujiwara are consultants of Oncolys BioPharma, Inc. No potential conflicts of interest were disclosed by the other authors.

Funding

This study was supported by grants from the Ministry of Health, Labor, and Welfare of Japan (to T. Fujiwara; No. 10103827, No. 13801426, No. 14525167) and by grants from the Ministry of Education, Culture, Sports, Science and Technology, Japan (T. Fujiwara; No. 25293283).

Dedication

This paper is dedicated to the memory of A.R. Moossa, M.D. and Sun Lee, MD.

References

[1] American Cancer Society. Cancer Facts & Figures 2016. 2016, American Cancer Society: Atlanta
[2] Slominski AT, Carlson JA. Melanoma resistance: bright future for academicians and challenge for patient advocates. Mayo Clin Proc 2014; 89:429-433; PMID:24684870; https://doi.org/10.1016/j.mayocp.2014.02.009
[3] Kawczyk-Krupka A, Bugaj AM, Latos W, Zaremba K, Sieroń A. Photodynamic therapy in treatment of cutaneous and choroidal melanoma. Photodiagnosis Photodyn Ther 2013; 10:503-509; PMID:24284103; https://doi.org/10.1016/j.pdpdt.2013.05.006
[4] Lo JA, Fisher DE. The melanoma revolution: from UV carcinogenesis to a new era in therapeutics. Science 2014; 346:945-949; PMID:25414302; https://doi.org/10.1126/science.1253735
[5] Vera RE, Lamberti MJ, Rivarola VA, Rumie Vittar NB. Developing strategies to predict photodynamic therapy outcome: the role of melanoma microenvironment. Tumour Biol 2015; 36:9127-9136; PMID:26419592; https://doi.org/10.1007/s13277-015-4059-x
[6] Kawaguchi K, Murakami T, Chmielowski B, Igarashi K, Kiyuna T, Unno M, Nelson SD, Russell TA, Dry SM, Li Y, et al. Vemurafenib-resistant BRAF-V600E mutated melanoma is regressed by MEK targeting drug trametinib, but not cobimetinib in a patient-derived orthotopic xenograft (PDOX) mouse model. Oncotarget in press; https://doi.org/10.18632/oncotarget.12328
[7] Castano AP, Mroz P, Hamblin MR. Photodynamic therapy and anti-tumour immunity. Nat Rev Cancer 2006; 6:535-545; PMID:16794636
[8] Agostinis P, Berg K, Cengel KA, Foster TH, Girotti AW, Gollnick SO, Hahn SM, Hamblin MR, Juzeniene A, Kessel D, et al. Photodynamic therapy of cancer: an update. CA Cancer J Clin 2011; 61:250-281; PMID:21617154
[9] Kimura H, Lee C, Hayashi K, Yamauchi K, Yamamoto N, Tsuchiya H, Tomita K, Bouvet M, Hoffman RM. UV light killing efficacy of fluorescent protein-expressing cancer cells *in vitro* and *in vivo*. J Cell Biochem 2010; 110:1439-1446; PMID:20506255; https://doi.org/10.1002/jcb.22693
[10] Tsai M-H, Aki R, Amoh Y, Hoffman RM, Katsuoka K, Kimura H, Lee C, Chang C-H. GFP-fluorescence-guided UVC irradiation inhibits melanoma growth and angiogenesis in nude mice. Anticancer Res 2010; 30:3291-3294; PMID:20944099
[11] Momiyama M, Suetsugu A, Kimura H, Kishimoto H, Aki R, Yamada A, Sakurada H, Chishima T, Bouvet M, Bulgakova NN, et al. Fluorescent proteins enhance UVC PDT of cancer cells. Anticancer Res 2012; 32:4327-4330; PMID:23060554
[12] Momiyama M, Suetsugu A, Kimura H, Kishimoto H, Aki R, Yamada A, Sakurada H, Chishima T, Bouvet M, Endo I, et al. Imaging the efficacy of UVC irradiation on superficial brain tumors and metastasis in live mice at the subcellular level. J Cell Biochem 2013; 114:428-434; PMID:22961687; https://doi.org/10.1002/jcb.24381
[13] Hiroshima Y, Maawy A, Zhang Y, Sato S, Murakami T, Yamamoto M, Uehara F, Miwa S, Yano S, Momiyama M, et al. Fluorescence-guided surgery in combination with UVC irradiation cures metastatic human pancreatic cancer in orthotopic mouse models. PLoS One 2014; 9:e99977; PMID:24924955; https://doi.org/10.1371/journal.pone.0099977
[14] Takehara K, Tazawa H, Okada N, Hashimoto Y, Kikuchi S, Kuroda S, Kishimoto H, Shirakawa Y, Narii N, Mizuguchi H, et al. Targeted photodynamic virotherapy armed with a genetically encoded photosensitizer. Mol Cancer Ther 2016; 15:199-208; PMID:26625896; https://doi.org/10.1158/1535-7163.MCT-15-0344
[15] Shirmanova MV, Serebrovskaya EO, Lukyanov KA, Snopova LB, Sirotkina MA, Prodanetz NN, Bugrova ML, Minakova EA, Turchin IV, Kamensky VA, et al. Phototoxic effects of fluorescent protein KillerRed on tumor cells in mice. J Biophotonics 2013; 6:283-290; PMID:22696211; https://doi.org/10.1002/jbio.201200056
[16] Kikuchi S, Kishimoto H, Tazawa H, Hashimoto Y, Kuroda S, Nishizaki M, Nagasaka T, Shirakawa Y, Kagawa S, Urata Y, et al. Biological ablation of sentinel lymph node metastasis in submucosally invaded early gastrointestinal cancer. Mol Ther 2015; 23:501-509; PMID:25523761; https://doi.org/10.1038/mt.2014.244
[17] Kojima T, Watanabe Y, Hashimoto Y, Kuroda S, Yamasaki Y, Yano S, Ouchi M, Tazawa H, Uno F, Kagawa S, et al. In vivo biological purging for lymph node metastasis of human colorectal cancer by telomerase-specific oncolytic virotherapy. Ann Surg 2010; 251:1079-1086; PMID:20485131; https://doi.org/10.1097/SLA.0b013e3181deb69d
[18] Yano S, Takehara K, Kishimoto H, Urata Y, Kagawa S, Bouvet M, Fujiwara T, Hoffman RM. Adenoviral targeting of malignant melanoma for fluorescence-guided surgery prevents recurrence in orthotopic nude-mouse models. Oncotarget 2016; 7(14):18558-72, Epub ahead of print; https://doi.org/10.18632/oncotarget.6670
[19] Yano S, Miwa S, Kishimoto H, Urata Y, Tazawa H, Kagawa S, Bouvet M, Fujiwara T, Hoffman RM. Eradication of osteosarcoma by fluorescence-guided surgery with tumor labeling by a killer-reporter adenovirus. J Orthopaedic Res 2016; 34:836-844; https://doi.org/10.1002/jor.23073
[20] Yano S, Takehara K, Miwa S, Kishimoto H, Hiroshima Y, Murakami T, Urata Y, Kagawa S, Bouvet M, Fujiwara T, et al. Improved resection and outcome of colon-cancer liver metastasis with fluorescence-guided surgery using in situ GFP labeling with a telomerase-dependent adenovirus in an orthotopic mouse model. PLoS One 2016; 11:e0148760; PMID:26849435

[21] Yano S, Zhang Y, Miwa S, Kishimoto H, Urata Y, Bouvet M, Kagawa S, Fujiwara T, Hoffman RM. Precise navigation surgery of tumours in the lung in mouse models enabled by in situ fluorescence labelling with a killer-reporter adenovirus. BMJ Open Respir Res 2015; 2:e000096; PMID:26380093; https://doi.org/10.1136/bmjresp-2015-000096

[22] Yano S, Miwa S, Kishimoto H, Uehara F, Tazawa H, Toneri M, Hiroshima Y, Yamamoto M, Urata Y, Kagawa S, et al. Targeting tumors with a killer-reporter adenovirus for curative fluorescence-guided surgery of soft-tissue sarcoma. Oncotarget 2015; 6:13133-13148; PMID:26033451

[23] Yano S, Miwa S, Kishimoto H, Toneri M, Hiroshima Y, Yamamoto M, Bouvet M, Urata Y, Tazawa H, Kagawa S, et al. Experimental curative fluorescence-guided surgery of highly invasive glioblastoma multiforme selectively labeled with a killer-reporter adenovirus. Mol Therapy 2015; 23:1182-1188; PMID:25896244; https://doi.org/10.1038/mt.2015.63

[24] Slominski A, Zbytek B, Slominski R. Inhibitors of melanogenesis increase toxicity of cyclophosphamide and lymphocytes against melanoma cells. Int J Cancer 2009; 124:1470-1477; PMID:19085934; https://doi.org/10.1002/ijc.24005

[25] Slominski RM, Zmijewski MA, Slominski AT. The role of melanin pigment in melanoma. Exp Dermatol 2015; 24:258-259; PMID:25496715

[26] Broż yna AA, Jóźwicki W, Roszkowski K, Filipiak J, Slominski AT. Melanin content in melanoma metastases affects the outcome of radiotherapy. Oncotarget 2016; 7:17844-17853; PMID:26910282; https://doi.org/10.18632/oncotarget.7528

[27] Blagosklonny MV. Matching targets for selective cancer therapy. Drug Discov Today 2003; 8:1104-1107; PMID:14678733

[28] Blagosklonny MV. Teratogens as anti-cancer drugs. Cell Cycle 2005;4:1518-1521; PMID:16258270

[29] Blagosklonny MV. Treatment with inhibitors of caspases, that are substrates of drug ransporters, selectively permits chemotherapy-induced apoptosis in multidrug-resistant cells but protects normal cells. Leukemia 2001; 15:936-941; PMID:11417480

[30] Blagosklonny MV. Target for cancer therapy: proliferating cells or stem cells. Leukemia 2006; 20:385-391; PMID:16357832; https://doi.org/10.1038/sj.leu.2404075

[31] Apontes P, Leontieva OV, Demidenko ZN, Li F, Blagosklonny MV. Exploring long-term protection of normal human fibroblasts and epithelial cells from chemotherapy in cell culture. Oncotarget 2011; 2:222-233; PMID:21447859; https://doi.org/10.18632/oncotarget.248

[32] Blagosklonny MV. Tissue-selective therapy of cancer. Br J Cancer 2003; 89:1147-1151; PMID:14520435

[33] Bobek V, Kolostova K, Pinterova D, Kacprzak G, Adamiak J, Kolodziej J, Boubelik M, Kubecova M, Hoffman RM. A clinically relevant, syngeneic model of spontaneous, highly metastatic B16 mouse melanoma. Anticancer Res 2010; 30:4799-4803; PMID:21187455

[34] Hoffman RM, Yang M. Subcellular imaging in the live mouse. Nat Protocols 2006; 1:775-782; PMID:17406307

[35] Hoffman RM, Yang M. Color-coded fluorescence imaging of tumor-host interactions. Nat Protocols 2006; 1:928-935; PMID:17406326; https://doi.org/10.1038/nprot.2006.119

[36] Hoffman RM, Yang M. Whole-body imaging with fluorescent proteins. Nat Protocols 2006; 1:1429-1438; PMID:17406431

[37] Yamauchi K, Yang M, Jiang P, Xu M, Yamamoto N, Tsuchiya H, Tomita K, Moossa AR, Bouvet M, Hoffman RM. Development of real-time subcellular dynamic multicolor imaging of cancer cell trafficking in live mice with a variable magnification whole-mouse imaging system. Cancer Res 2006; 66:4208-4214; PMID:16618743; https://doi.org/10.1158/0008-5472.CAN-05-3927